Available online at www.sciencedirect.com
SCIENCE DIRECT®
Journal of Process Control 16 (2006) 409–417
JOURNAL OF PROCESS CONTROL
www.elsevier.com/locate/jprocont

# Robust nonlinear feedback–feedforward control of a coupled kinetic Monte Carlo–finite difference simulation

Effendi Rusli, Timothy O. Drews, David L. Ma, Richard C. Alkire, Richard D. Braatz *

*Department of Chemical and Biomolecular Engineering, University of Illinois at Urbana-Champaign, 600 South Mathews Avenue, 93 Roger Adams Laboratory, Box C-3, Urbana, IL 61801, USA*

Received 14 September 2004; received in revised form 28 March 2005; accepted 9 May 2005

**Abstract**

Robust nonlinear feedforward–feedback controllers are designed for a multiscale system that dynamically couples kinetic Monte Carlo (KMC) and finite difference (FD) simulation codes. The coupled codes simulate the copper electrodeposition process for manufacturing on-chip copper interconnects in electronic devices. The control objective is to regulate the current density subject to the condition that the steady-state fluctuation of the overpotential remains bounded within ±0.01 V. The controller designs incorporate a low-order stochastic model that captures the input–output behavior of the coupled KMC–FD code. The controllers achieve the objectives and the closed-loop responses implemented on the low-order model and the coupled KMC–FD code match well within stochastic variations. The nonlinear feedforward control reduces the rise time of the controller response while the feedback control ensures robustness in the presence of model uncertainty.


*Keywords:* Stochastic simulation; Noncontinuum models; Kinetic Monte Carlo simulation; Nonlinear control; Gain-scheduled control; Stochastic control; Markov processes; Finite differences

## 1. Introduction

The vast majority of the literature on controller design is based on continuum models, which are described by systems of algebraic, ordinary differential, and partial differential equations [26,29,30,42]. The continuum modeling approach, however, is inadequate for modeling much of the molecular, nanoscopic, and mesoscale phenomena that occur in the complex chemical processes that constitute the attention of today's scientists and engineers [9,35,50,51]. This is especially apparent in microelectronics processes, for which the most interesting phenomena occur at the nanometer and smaller length scales [24]. Hence in recent years increasing efforts have been directed towards the development of noncontinuum models, such as kinetic Monte Carlo (KMC) simulation models [8,9,18,21,23,51,52], for which most controller design techniques are not directly applicable. Actually, it is only recently that the higher level *analysis* of such stochastic simulators has been possible, and only then applicable to certain classes of simulated processes, such as those with a clear separation of time scales [34,44,49].

Global competition has increased the importance of feedback control for the complex chemical processes that are best described by noncontinuum models. There is probably no place where this is more apparent than in the semiconductor industry, which has had an average annual growth of 20%, with sales of $200 billion in 2001. It is generally accepted that high performance control will be required to achieve the small length scales

* Corresponding author. Tel.: +1 217 333 5073; fax: +1 217 333 5052.
*E-mail address:* braatz@uiuc.edu (R.D. Braatz).

0959-1524/$ - see front matter © 2005 Elsevier Ltd. All rights reserved.
doi:10.1016/j.jprocont.2005.05.007

required to provide high computational speed in future electronic devices [47].

The design of feedback controllers based on such noncontinuum models is one of the most challenging open research problems in the field of control [40]. For KMC codes, it has been proposed to construct reduced-order models by truncating unlikely configurations and grouping probabilities that evolve together [14–16], using smaller lattices [31,32], or applying time-steppers [4,48] or least-squares systems identification methods [13,17]. Similar reduced-order models have been defined for dynamically coupled continuum/noncontinuum codes [41,46].

Here a feedforward–feedback controller is designed for a coupled kinetic Monte Carlo–finite difference (KMC–FD) code that simulates the electrochemical deposition of copper into a trench, which is a key process step in manufacturing on-chip interconnects for microelectronic devices [2,19]. The industrial need is to deposit copper uniformly into trenches and vias of small dimension (less than 100 nm) under galvanostatic (i.e., constant current) conditions. This industrial importance has motivated numerous experimental and simulation studies on the modeling of copper electrodeposition in recent years [1,3,20,22,25,36–38]. The goal of the feedforward–feedback controller is to maintain the current or current density at a constant specified value, without creating large fluctuations in the applied overpotential. The controller enables the coupled KMC–FD simulations to operate under experimental operating conditions so that a separate study, outside the scope of this paper, can be done to compare model predictions from the coupled KMC–FD codes to the collected data.

The paper is organized as follows. First, the coupled KMC–FD copper electrodeposition simulation code is described. This is followed by construction of a low-order stochastic model that is used to design feedforward–feedback controllers and gain-scheduled filters to handle the nonGaussian stochastic noise produced by the KMC code. Then the closed-loop responses of the controllers are compared in simulations of the low-order stochastic model and the KMC–FD simulation code.

## 2. Coupled kinetic Monte Carlo–finite difference simulation code

Kinetic Monte Carlo (KMC) methods are used to simulate structural properties of matter that are not completely describable by a macroscopic continuum description, and are increasingly used for simulating chemical and materials processes. A KMC simulation is a realization of the Master equation [12,28]:

$$\frac{\partial P(\sigma,t)}{\partial t} = \sum_{\sigma'} W(\sigma',\sigma)P(\sigma',t) - \sum_{\sigma'} W(\sigma,\sigma')P(\sigma,t) \quad (1)$$

where $\sigma$ and $\sigma'$ are successive states of the system, $P(\sigma,t)$ is the probability that the system is in state $\sigma$ at time $t$, $W(\sigma',\sigma)$ is the probability per unit time that the system will undergo a transition from $\sigma'$ to $\sigma$, and the state $\sigma$ refers to an allowable set of locations for all atoms in the system. The Master equation is a conservation equation for the probability that a system is in state $\sigma$, with the first and second terms on the right hand side of (1) being the total probabilities for a move into and out of the state $\sigma$, respectively. Directly integrating the differential Eq. (1) for all of the states is infeasible, since the total number of differential equations, one for each state, is too large. Instead, only a single realization is computed, in which the KMC code chooses randomly among the possible transitions of the system and accepts particular transitions with appropriate probabilities. After each accepted or attempted transition, the time variable is incremented by one Monte Carlo time step, and the process is repeated. The probabilities are selected to satisfy certain conditions [12] that ensure that the real time variable $t$ can be computed that corresponds to the number of Monte Carlo time steps.

The electrochemical deposition of copper into a trench is simulated in this application. A KMC method was used to simulate the processes on the surface, which enables the computation of the evolution of the surface roughness, which is an important characteristic of the produced copper deposit. The FD code describes the processes occurring within the fluid boundary layer above the MC domain. The FD and KMC codes are described only in enough detail to explain the control problem, with more detailed descriptions provided elsewhere [10].

The experimental system used for deposition is a rotating disk electrode, where the substrate is attached to the disk and immersed in the electrolytic solution, resulting in the electrode facing downward into the solution. The rotation of the disk causes a surface boundary layer to form that extends from the substrate surface to several microns into the electrolyte and the thickness of the layer is controlled by the disk rotation rate. It has been shown that the dominant method of transport to the surface is by diffusion. A 1D continuum FD code was used to simulate diffusion of cupric ions only through the surface boundary layer [10]. The continuum model is an explicit finite difference solution to the diffusion equation

$$\frac{\partial C_k}{\partial t} = D_k \frac{\partial^2 C_k}{\partial z^2} \quad (2)$$

where $C_k$ and $D_k$ are the concentration and diffusion coefficient for species $k$, respectively, and $z$ is the distance above the surface. The boundary conditions used for solution were the concentration at the KMC–FD interface that was updated each time the codes communicated, and a constant concentration boundary condi-

tion in the bulk. The height of the continuum domain was set to 50 μm, which is close to the diffusion boundary layer thickness under typical processing conditions.

The KMC code describes the mesoscale with a cubic lattice, where each subdomain in the simulation space represents clusters of molecules (referred to as a mesoparticle) of a given species in the deposition bath (see Fig. 1). Each cubic subdomain is 12.5 nm on a side and is assumed to be homogeneous in both phase and composition. Similar coarse-grained mesoscale KMC approaches have been applied by various researchers to a number of systems [e.g., 5,6,10,11,27,33]. While truly molecular-scale simulations are of interest, this coarser mesoscale representation results in an efficient computational method that can predict surface roughness on the same scale as is measured experimentally [10,11]. The T-shaped Monte Carlo domain consists of a trench with aspect ratio 2:1, with the trench being 40 subdomains wide, 80 subdomains high, and 6 subdomains deep. The top of the simulation domain is 70 subdomains wide.

The Monte Carlo domain has periodic boundary conditions in the $x$ and $y$ directions, an impenetrable boundary at the electrode surface (in the $z$ direction), and receives mass fluxes at the top boundary in the $z$ direction from the FD code. The KMC code provides the species concentrations to the continuum code. The KMC code also reads an applied overpotential $\eta$ as input and produces a signal that is the charge passed during deposition. These signals serve as the output and input of the feedback controller (see Fig. 1). This paper considers the case where only pure copper and its charge forms are simulated. It should be noted that the use of solution additives is critically important for achieving a desired time-evolution of the deposit shape, but are not considered in this treatment. The extension of the control technique established here to more sophisticated simulations involving additive effects is straightforward, since tracking additional chemical species does not affect significantly the control problem or design methodology. Almost all of the charge that is passed is associated with reduction of copper.

The KMC code simulates deposition phenomena by considering the likelihood of various actions that each mesoparticle can take at a given time step. These actions are bulk diffusion, adsorption, desorption, and surface diffusion and reaction. All actions are computed as frequencies, with units of $s^{-1}$. At a given Monte Carlo time step, a mesoparticle can make a maximum of one move. The moves that each mesoparticle can make are specified in an input file. The possible moves that each species can make are a function of the location of the mesoparticle in the simulation space, as well as the number and type of the six nearest neighbors.

Three time steps are tracked in the KMC simulation code: (1) the time step over which the FD code is called for updated flux information (the linking time step); (2) the sampling interval for the feedback controller; and (3) the Monte Carlo (MC) time step. In order to capture the full dynamics of the system, the MC time step must be small enough to capture the most frequent actions. In this copper electrodeposition application, the Monte Carlo time step was computed to be ~2.8 ns, from Eq. (7) of [10]. A complete KMC simulation run typically requires $1.08 \times 10^8$ MC time steps before the copper film reaches its desired thickness. In this particular study, the linking time step and the sampling interval for the controller are set to be $10^{-7}$ s and $10^{-2}$ s, respectively. The magnitude of the linking time step was selected small enough to ensure stability in the interconnected systems [10], while being large enough that the overall computational expense is manageable.

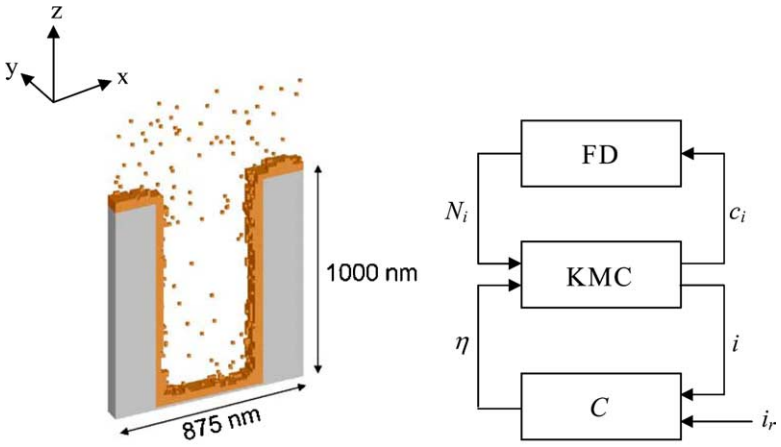


Fig. 1. Simulation coupling of the KMC–FD codes with a controller. FD denotes finite difference code, KMC denotes kinetic Monte Carlo code, and C is the controller. The KMC domain is illustrated on the left. At each linking time step, the KMC code passes the species concentration $c_i$ at the interface to the FD code and in return, the FD code passes the species flux $N_i$ at the interface to the KMC code. The control output is current density $i$, the manipulated variable is the overpotential $\eta$, and $i_r$ is the controller set point.

To carry out the galvanostatic (i.e., constant current) simulations associated with industrial plating operations, the controller must manipulate the applied overpotential $\eta$ to control the current density $i$, based on the charge transferred as a function of time. There are two main requirements for the controller. First, the controller should have a tracking response as fast as possible, preferably with a settling time of less than 1 s. Second, the manipulated variable should not have overly large fluctuations (within $\pm 0.01$ V). The applied overpotential $\eta$ enters the surface reaction frequencies in a highly nonlinear manner. This suggests that nonlinear control may give better performance than linear control. The next section describes how a low-order stochastic model was constructed from input–output data collected from the KMC–FD code.

## 3. Identification of low-order stochastic and deterministic models

The KMC–FD code is computationally expensive, highly stochastic, and nonlinear. To design low-order controllers, a low-order stochastic model was constructed that captured the most essential input–output behavior of the coupled KMC–FD code. This low-order model was incorporated into model-based controller design and used for filter and controller tuning.

The output of the KMC–FD code was the cumulative charge passed from the beginning of the simulation up to the current simulation time. To emulate the real physical system as closely as possible, the charge signal was converted to a current density signal. The current density was computed as the total charge passed in every 0.01 second per $cm^2$ of surface area. A larger time step interval could be used to compute the current from the charge, but this would lead to a more sluggish response, causing an inherent performance limitation in the controller. On the other hand, decreasing the time step leads to a more highly noise-corrupted signal. The manipulated variable is the applied overpotential, which affects the kinetics of the mechanisms simulated in the KMC–FD code and hence directly affects the current generation.

The model identification stage consisted of applying a series of step input overpotentials to the KMC–FD code within the operation conditions of the code and observing the current densities. Sample results are plotted in Fig. 2. Comparison of the probability mass function of different time segments suggests that each step response reaches steady state immediately. This is not surprising since the simulation time step for the KMC–FD code is much smaller than the time step of the control action. The KMC and FD codes are linked dynamically and communicate to each other by passing boundary conditions every $10^{-7}$ s, which is five orders of magnitude smaller than the time step of the control action.

The stochastic fluctuations displayed in the output response are nonGaussian and asymmetric, and can be modeled by a discrete Poisson distribution for all normal operating conditions. To ensure consistency and accuracy, the identification procedure was repeated with different seed numbers. These sets of input–output data were used in the parameter estimation of a low-order stochastic model:

$$P(i(k) = \kappa | \eta(k-1)) = \frac{\lambda^{-400\kappa} e^{-\lambda}}{(-400\kappa)!} \tag{3}$$

$$\lambda = 2.5285 e^{-6.5962\eta(k-1)} - 1.3622 \tag{4}$$

where $k$ is the time index ($k \in Z$, where $Z$ is the set of nonnegative integers), $\kappa \in \{-0.0025n, n \in Z\}$, $\eta$ is the overpotential, and $i(k)$ is the observed current density. The incremental value of $\kappa$ is affected by the amount of charges involved in the reduction of copper species contained in one cubic lattice (subdomain). The form of the nonlinearity was motivated by the expression for the surface kinetics [10]. Fig. 3 compares the stochastic current density produced by the low-order model (3) and (4) and the KMC–FD code for a range of applied overpotential.

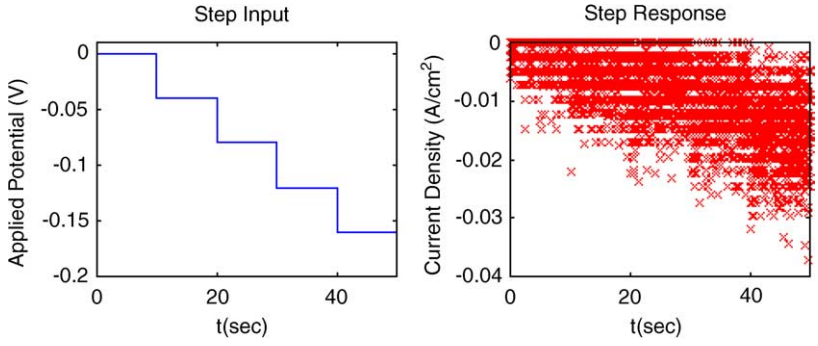


Fig. 2. Incremental step input implemented on the KMC–FD code and the resulting step response. The step response was constructed by plotting the current density computed by dividing the sum of charge passed in each 0.01 s interval by 0.01 s and the surface area. The amount of charge passed is proportional to the amount of copper deposited.

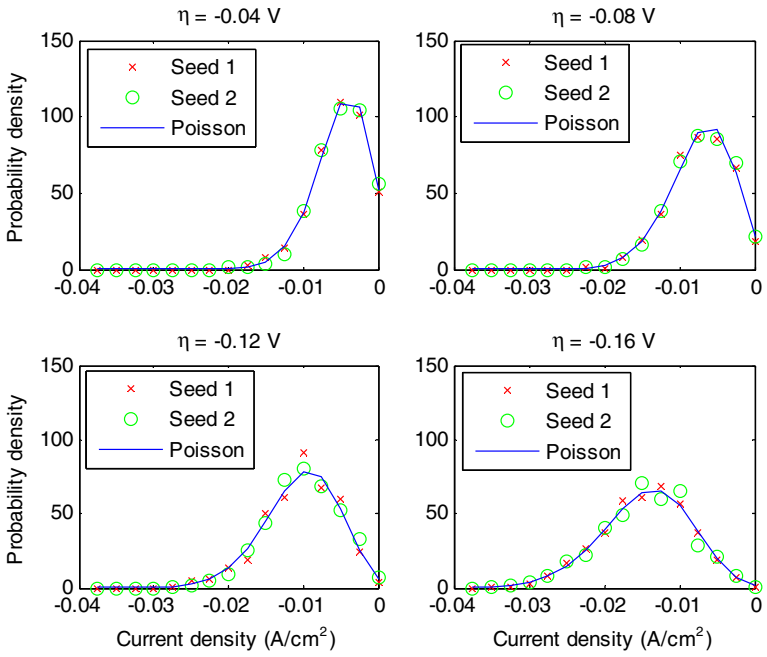


Fig. 3. Current density distributions for four distinct input overpotential $\eta$ values for the low-order stochastic model (3) and (4) (solid line) and the coupled KMC–FD simulation (× and ○ correspond to simulation data with different seed numbers).

## 4. Controller and filter designs

Linear, gain-scheduled, and nonlinear controllers were designed based on the low-order stochastic model (3) and (4). Each controller incorporates a first-order filter (see Fig. 4):

$$F(z) = \frac{\alpha}{1-(1-\alpha)z^{-1}} \tag{5}$$

with filter coefficient $\alpha$. This filter serves two purposes. First, it reduces fluctuations in the manipulated variable without filtering the reference signal. Second, it increases the robust stability of the closed-loop system. The linear and nonlinear feedback controllers were initially designed based on the deterministic part of the low-order model (3) and (4) and then detuned using the filter (5) to meet the performance specifications. The deterministic model of the plant, which is the expected value of the current density as a function of the overpotential, was calculated from (3) and (4).

$$i(k) = -6.3213 \times 10^{-3} e^{-6.5962\eta(k-1)} + 3.4055 \times 10^{-3} \tag{6}$$

An alternative deterministic model, which schedules the mean process gain as a function of the input variable $\eta$,

$$i(k) = K\eta(k-1) \tag{7a}$$

can be derived from the step response data. The mean process gain was computed with respect to the steady-state condition at $\eta = 0$. The minimum least-squares fit to a quadratic function of the scheduled gain (see Fig. 5) was:

$$K = 4.6058\eta^2 + 0.22074\eta + 0.061912 \tag{7b}$$

The two deterministic models (6) and (7) give almost the same output prediction error over the full range of operating conditions.

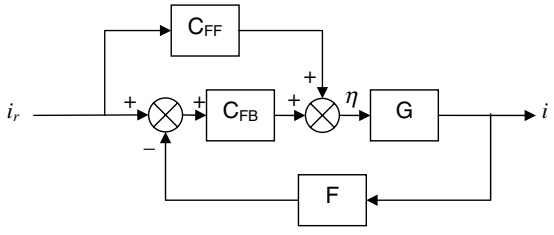


Fig. 4. Block diagram for the closed-loop system: $G$ is the plant (either the coupled KMC–FD codes or the low-order stochastic model), $C_{FB}$ and $C_{FF}$ are the feedback and feedforward controllers, $F$ is the filter, $\eta$ is the applied overpotential, $i$ is the current density, and $i_r$ is the desired current density.

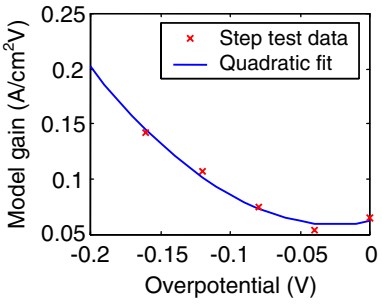


Fig. 5. Model gain $K$ for the KMC–FD simulation code computed from step data.

### 4.1. Feedback–feedforward controller designs

The gain in (7) varies by nearly a factor of three depending on the operating condition:

$$K \in [0.05, 0.1417] \tag{8}$$

where the upper bound was selected to exceed slightly the steady-state value for regulating the current density at $-0.015$ A/cm$^2$. The linear feedback controller was designed using internal model control [39]. The desired closed-loop response was first-order-plus-time-delay:

$$\frac{i}{i_r} = GC_{\mathrm{FB}}(1 + FGC_{\mathrm{FB}})^{-1} = \frac{(1 - \mathrm{e}^{-\Delta t/\tau})z^{-1}}{1 - \mathrm{e}^{-\Delta t/\tau}z^{-1}} \tag{9}$$

where $G$ is the process model, $C_{\mathrm{FB}}$ is the feedback controller, $\tau$ is the desired closed-loop time constant, $i_r$ is the desired current density, and $\Delta t$ is the controller sampling time. For the low-order model, $G = Kz^{-1}$, Eq. (9) was rearranged to derive the feedback controller

$$C_{\mathrm{FB}} = \frac{(1-\phi) - (1-\alpha)(1-\phi)z^{-1}}{1 - (1 + \phi(1-\alpha))z^{-1} + \phi(1-\alpha)z^{-2}} \cdot \frac{1}{K} \tag{10}$$

where $\phi = \mathrm{e}^{-\Delta t/\tau}$ and $\alpha$ is the filter coefficient. The model gain $K$ was chosen to be 0.1417 to obtain optimal performance for the operating conditions simulated in the paper while ensuring robust stability to the model gain variation in (8), using the sufficient condition for nonlinear time-varying perturbations in [7]. The values $\Delta t = 0.01$ s and $\tau = 10^{-5}$ s ensure fast response yet not faster than the dynamics of the KMC–FD simulation which is on the order of $10^{-6}$ s. The tuning of the filter coefficient $\alpha$ to satisfy closed-loop objectives is discussed in the next section.

The feedforward controller is designed based on the plant model in (6):

$$\eta = -\frac{1}{6.5962} \ln\left(\frac{3.4055 \times 10^{-3} - i_r}{6.3213 \times 10^{-3}}\right) \tag{11}$$

The feedforward term acts an inverter to cancel the static nonlinearity in the low-order model. As a result, the model combined with the inverter is a pure time delay with a unit gain. The fact that the nonlinearity is static for the nominal model causes the nonlinear robustness analysis to be straightforward and identical to the analysis reported by [43] for single-input single-output processes with linear dynamics and static nonlinearities.

Gain-scheduled and nonlinear inversion-based feedback controllers were also designed, but the closed-loop performances were very similar to that obtained by the linear feedback controller, and so for brevity those controller designs and closed-loop simulation results are not reported here. Interested readers are directed to a Masters thesis [45].

### 4.2. Gain-scheduled filter designs

The filter coefficient $\alpha$ was tuned to ensure that at least 90% of the fluctuations in the applied overpotential were within $\pm 0.01$ V over the entire operating regime, while avoiding too much filtering which leads to unnecessarily sluggish response. If a fixed filter coefficient were used, then it would have to be designed based on the probability density distribution of the applied overpotential at the final time, that is, the time required to fill up the trench with copper. The reason for this is that the applied overpotential is the most negative at the final time, and the stochastic fluctuations are largest when the applied overpotential is the most negative. A filter coefficient that adequately filters the stochastic fluctuations at the final time would also provide adequate filtering at earlier times, but would provide much more filtering than needed at the earlier times. This motivated the use of a gain-scheduled filter coefficient designed so that 90% of the fluctuations in the applied overpotential are within $\pm 0.01$ V regardless of the operating conditions.

A primary goal of this study was to create a filter and controller design procedure that can be quickly repeated when physicochemical parameters in the KMC–FD code are changed. Due to the high computational cost of running the KMC–FD code, its use in filter and controller design is limited to the creation of data for constructing the low-order stochastic model (3) and (4). The low-order stochastic model is then used to design the filter and controller. The approximate probability density distribution of the applied overpotential at the final time was obtained by running the closed-loop simulation using the low-order stochastic model with the selected feedback controller 10,000 times for several $\alpha$ values. The implementation of this Monte Carlo technique was fast. It took less than 4 min to complete 10,000 runs for one $\alpha$ value when the code is written in Microsoft Fortran and run on a Personal Computer with a 900 MHz Athlon processor. From this probability density distribution, the mean and 90% confidence interval were estimated. As discussed above, the values for the filter coefficient were determined which resulted in 90% of the fluctuations being within $\pm 0.01$ V for all values of the applied overpotential (which is directly related to the current density, through (6)). The least-squares fit mapping for a linear controller is given by

$$\alpha = 0.0923\mathrm{e}^{329.7 i_r} + 0.036 \tag{12}$$

where $i_r$ is the desired current density. Eq. (12) implies that within the normal operating regime, more filtering is required for larger current density. This result agrees with physical intuition as the variance of the process output variable increases with its mean value as shown in Fig. 2.

## 5. Results and discussion

Fig. 6 shows agreement between the closed-loop responses obtained by applying the feedforward–feedback controllers to the KMC–FD code and the low-order stochastic model (3) and (4), where the reference current density was $-0.015$ A/cm$^2$. The close agreement indicates that the low-order stochastic model was sufficiently accurate in capturing the stochastic behavior of the KMC–FD code that it could be used in filter design. As specified, the applied overpotential was within $\pm 0.01$ V of its steady-state value 90% of the time. Furthermore, the benefit of using the feedforward controller is demonstrated in Fig. 6 where the closed-loop response of the overpotential immediately becomes close to its steady state value. The feedforward–feedback controller has vastly superior closed-loop responses than the purely feedback controllers investigated in a previous study [46]. The high stochasticity of the current density computed by the KMC code greatly limits the closed-loop performance obtainable by a purely feedback controller, due to the limit on the allowed fluctuations in the manipulated variable (the applied overpotential). The speed of response of the feedforward controller is not limited by these stochastic fluctuations. The integral action in the feedback controller makes small corrections in the manipulated variable so that zero bias in the current density occurs at long time, under model uncertainty.

Fig. 7 shows that the feedforward–feedback controller successfully regulates the filtered current density to the desired setpoint. Again, a good agreement is observed for the closed-loop response of the filtered current density for the controller implemented on the low-order model (3) and (4) and the coupled KMC–FD code, indicating that the low-order model was sufficiently accurate to be used in controller design. Fig. 8 focuses on the initial time response of the filtered current density. The filtered current density reaches the desired set-point in less than 1 s for both the low-order model and the coupled KMC–FD codes.

Replacing the linear feedback controller with inversion-based nonlinear or gain-scheduled controllers [45] resulted in very similar closed-loop responses. This result is not surprising because the response at very short times is specified by the nonlinear feedforward controller, which was the same in all feedback–feedforward control designs, and the response at longer times is primarily specified by the dynamics of the filter $F$, which was the same in all feedback–feedforward control designs.

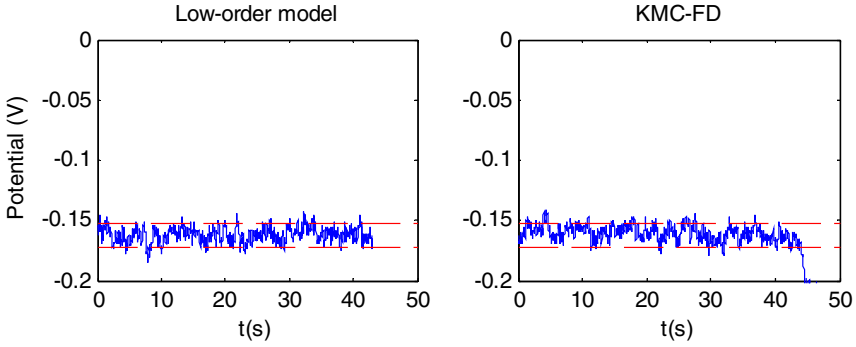


Fig. 6. Closed-loop response of the overpotential for the coupled feedforward and linear feedback controller implemented on the low-order stochastic model (3) and (4) and the KMC–FD simulation code.

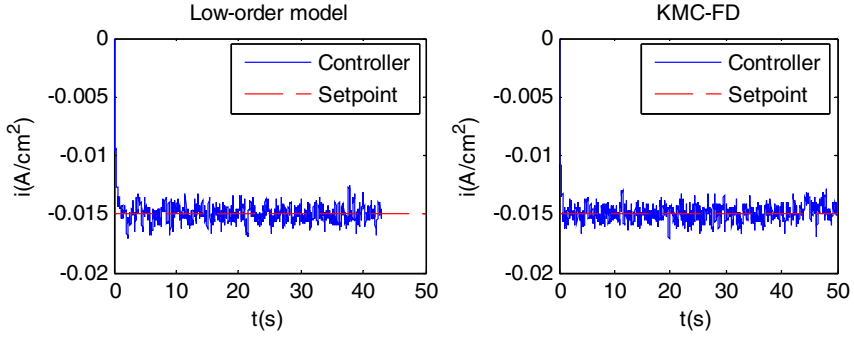


Fig. 7. Closed-loop response of the filtered current density for coupled feedforward and linear feedback controller implemented on the low-order stochastic model (3) and (4) and the KMC–FD simulation code.

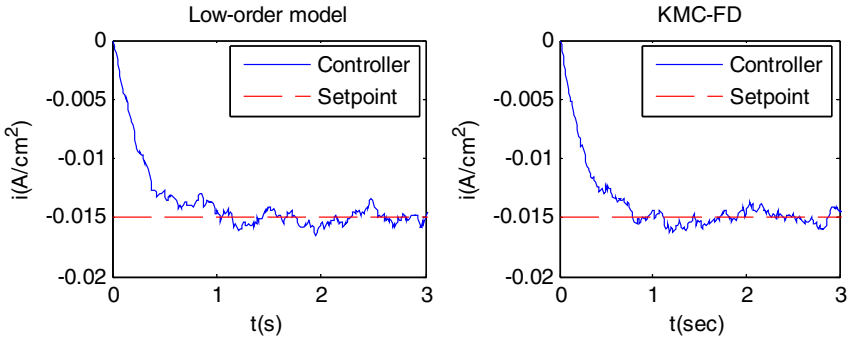


Fig. 8. Initial transient response of the filtered current density for the coupled feedforward and linear feedback implemented on the low-order stochastic model (3) and (4) and the KMC–FD simulation code.

## 6. Conclusions

A low-order feedforward–feedback controller was designed for a coupled kinetic Monte Carlo–finite difference code that simulates the infill of a trench during copper electrodeposition. The feedforward–feedback controller and associated gain-scheduled filter were constructed from a low-order stochastic model constructed from data collected from the KMC–FD code. The controller enables the KMC–FD code to operate under constant current conditions, which is typically done in industrial practice. The controller was also designed to keep the steady-state fluctuations of the overpotential bounded within $\pm 0.01$ V. Differences between the closed-loop simulations obtained with the low-order stochastic model and the KMC–FD code were within the stochastic variations in the responses, which justified the use of the low-order stochastic model for filter and controller design.

## Acknowledgements

The authors gratefully acknowledge support from the National Science Foundation (CTS-0135621, CTS-0438356, NRAC-MCA01S022). Any opinions, findings, and conclusions or recommendations expressed in this material are those of the authors and do not necessarily reflect the views of the National Science Foundation.

## References

[1] R.C. Alkire, E.D. Eliadis, Electrodeposition of copper: the effect of various organic compounds, Z. Physik. Chemie 208 (1999) 1–15.
[2] P.C. Andricacos, Copper on-chip interconnections: a breakthrough in electrodeposition to make better chips, Electrochem. Soc. Interface 8 (1999) 32–39.
[3] P.C. Andricacos, C. Uzoh, J.O. Dukovic, J. Horkins, H. Deligianni, Damascene copper electroplating for chip interconnections, IBM J. Res. Dev. 42 (1998) 567–574.
[4] A. Armaou, C.I. Siettos, I.A. Kevrekidis, Time-steppers and 'coarse' control of distributed parameter microscopic processes, Int. J. Robust Nonlinear Control 14 (2004) 89–111.
[5] G.A. Bird, Molecular Gas Dynamics and the Direct Simulation of Gas Flows, Clarendon Press, Oxford, 1994.
[6] C.K. Birdsall, A.B. Langdon, Plasma Physics via Computer Simulation, McGraw-Hill, New York, 1985.
[7] R. Braatz, M. Morari, A multivariable stability margin for systems with mixed time-varying parameters, Int. J. Robust Nonlinear Control 7 (1997) 105–112.
[8] D.G. Coronell, D.E. Hansen, A.F. Voter, C. Liu, X. Liu, J.D. Kress, Molecular dynamics-based ion-surface interaction models for ionized physical vapor deposition feature scale simulations, Appl. Phys. Lett. 73 (1998) 3860–3862.
[9] M.W. Deem, Recent contributions of statistical mechanics in chemical engineering, AIChE J. 44 (1998) 2569–2596.
[10] T.O. Drews, E.G. Webb, D.L. Ma, J. Alameda, R.D. Braatz, R.C. Alkire, Coupled mesoscale-continuum simulations of copper electrodeposition in a trench, AIChE J. 50 (2004) 226–240.
[11] T.O. Drews, R.D. Braatz, R.C. Alkire, Coarse-grained kinetic Monte Carlo simulation of copper electrodeposition with additives, Int. J. Multiscale Comput. Eng. 2 (2004) 313–327.
[12] K.A. Fichthorn, W.H. Weinberg, Theoretical foundations of dynamic Monte-Carlo simulations, J. Chem. Phys. 95 (1991) 1090–1096.
[13] M.A. Gallivan, Optimization, estimation, and control for kinetic Monte Carlo simulations of thin film deposition, in: Proceedings of the Conference on Decision and Control, IEEE Press, Piscat away, New Jersey, USA, 2003, pp. 3437–3442.
[14] M.A. Gallivan, H.A. Atwater, Design of a film surface roughness-minimizing molecular beam epitaxy process by reduced-order modeling of epitaxial growth, J. Appl. Phys. 95 (2004) 483–489.
[15] M.A. Gallivan, R.M. Murray, Model reduction and system identification for master equation control systems, in: Proceedings of the American Control Conference, IEEE Press, Piscataway, New Jersey, USA, 2003, pp. 3561–3566.
[16] M.A. Gallivan, R.M. Murray, Reduction and identification methods for Markovian control systems, with application to thin film deposition, Int. J. Robust Nonlinear Control 14 (2004) 113–132.
[17] M.A. Gallivan, R.M. Murray, D.G. Goodwin, The dynamics of thin film growth: a modeling study. in: Allendorf, M.D., Hitchman, M.L. (Eds.), CVD XV: Proceedings of the Fifteenth Symposium on Chemical Vapor Deposition, The Electrochemical Society, vol. 616, 2000, pp. 168–175.
[18] M.A. Gallivan, D.G. Goodwin, R.M. Murray, Modeling and control of thin film morphology using unsteady processing parameters: Problem formulation and initial results, in: Proceed-

ings of the IEEE Conference on Decision and Control, 2001, IEEE Press, Piscataway, NJ, pp. 1570–1576.

[19] W.C. Gau, T.C. Chang, Y.S. Lin, J.C. Hu, L.J. Chen, C.Y. Chang, C.L. Cheng, Copper electroplating for future ultra large scale integraton interconnection, J. Vac. Sci. Technol. A 18 (2000) 656–660.

[20] M. Georgiadou, D. Veyret, R.L. Sani, R.C. Alkire, Simulation of shape evolution during electrodeposition of copper in the presence of additive, J. Electrochem. Soc. 148 (2001) C54–C58.

[21] G.H. Gilmer, H. Huang, T.D. de la Rubia, J.D. Torre, F. Baumann, Lattice Monte Carlo models of thin film deposition, Thin Solid Films 365 (2000) 189–200.

[22] W.N. Gill, D.J. Duquette, D. Varadarajan, Mass transfer models for the electrodeposition of copper with a buffering agent, J. Electrochem. Soc. 148 (2001) C289–C296.

[23] D. Hadji, Y. Marechal, J. Zimmermann, Finite element and Monte Carlo simulation of submicrometer silicon n-MOSFET's, IEEE Trans. Magnetics 35 (1999) 1809–1812.

[24] U. Hansen, S. Rodgers, K.F. Jensen, Modeling of metal thin film growth: linking Angstrom-scale molecular dynamics results to micro-scale film topographies, Phys. Rev. B 62 (2000) 2869–2878.

[25] J.M.E. Harper, C. Cabral, P.C. Andricacos, L. Gignac, I.C. Noyan, K.P. Rodbell, C.K. Hu, Mechanisms for microstructure evolution in electroplated copper thin films near room temperature, J. Appl. Phys. 86 (1999) 2516–2525.

[26] M.A. Henson, D.E. Seborg (Eds.), Nonlinear Process Control, Prentice Hall, Upper Saddle River, NJ, 1997.

[27] M.A. Katsoulakis, A.J. Majda, D.G. Vlachos, Course-grained stochastic processes and Monte Carlo simulators for the diffusion of interacting particles, J. Chem. Phys. 119 (2003) 9412–9427.

[28] D.P. Landau, K. Binder, A Guide to Monte Carlo Simulations in Statistical Physics, Cambridge University Press, Cambridge, United Kingdom, 2000.

[29] W.S. Levine (Ed.), The Control Handbook, CRC Press, Boca Raton, FL, 1995.

[30] L. Ljung, System Identification: Theory for the User, Prentice-Hall, Englewood Cliffs, NJ, 1987.

[31] Y.M. Lou, P.D. Christofides, Estimation and control of surface roughness in thin film growth using kinetic Monte-Carlo models, Chem. Eng. Sci. 58 (2003) 3115–3129.

[32] Y.M. Lou, P.D. Christofides, Feedback control of growth rate and surface roughness in thin film growth, AIChE J 49 (2003) 2099–2113.

[33] J. Lu, M.J. Kushner, Trench filling by ionized metal physical vapor deposition, J. Vac. Sci. Technol. A 19 (2001) 2652–2663.

[34] A.G. Makeev, D. Maroudas, I.G. Kevrekidis, Course stability and bifurcation analysis using stochastic simulators: kinetic Monte Carlo examples, J. Chem. Phys. 116 (2002) 10083–10091.

[35] D. Maroudos, Multiscale modeling of hard materials: challenges and opportunities for chemical engineering, AIChE J. 46 (2000) 878–882.

[36] T.P. Merchant, M.K. Gobbert, T.S. Cale, L.J. Borucki, Multiple scale integrated modeling of deposition processes, Thin Solid Films 365 (2000) 368–375.

[37] T.P. Moffet, J.E. Bonevich, W.H. Huber, A. Stanishevsky, D.R. Kelly, G.R. Stafford, D. Josell, Superconformal electrodepositon of copper in 500–90 nm features, J. Electrochem. Soc. 147 (2000) 4524–4535.

[38] T.P. Moffet, D. Wheeler, W.H. Huber, D. Josell, Superconformal electrodeposition of copper, Electrochemical and Solid State Letters 4 (2001) C26–C29.

[39] M. Morari, E. Zafiriou, Robust Process Control, Prentice-Hall, Englewood Cliffs, NJ, 1989.

[40] R.M. Murray (Ed.), Control in an Information Rich World: Report of the Panel on Future Directions in Control Dynamics and Systems, SIAM Press, Philadelphia, PA, 2003, pp. 63–70.

[41] S. Raimondeau, D.G. Vlachos, Low-dimensional approximations of multiscale epi taxial growth models for microstructure control of materials, J. Comp. Phys. 160 (2000) 564–576.

[42] W.H. Ray, Advanced Process Control, McGraw-Hill, New York, 1981.

[43] E. Rios-Patron, R.D. Braatz, Robust nonlinear control of a pH neutralization process, in: Proceedings of the American Control Conference, 1999, IEEE Press, Piscataway, NJ, pp. 119–124.

[44] O. Runborg, C. Theodoropoulos, I.G. Kevrekidis, Effective bifurcation analysis: a time-stepper-based approach, Nonlinearity 15 (2002) 491–511.

[45] E. Rusli, Nonlinear control of a coupled kinetic Monte Carlo-finite difference simulation, M.S. thesis, 2003, University of Illinois, Urbana, IL.

[46] E. Rusli, T.O. Drews, D.L. Ma, R.C. Alkire, R.D. Braatz, Nonlinear feedback control of a coupled kinetic Monte Carlo-finite dif ference simulation, in: Proceedings of the IFAC Symposium on Advanced Control of Chemical Processes, Hong Kong, 2003, pp. 597–602.

[47] Sematech, International Technology Roadmap for Semiconductors. Semiconductor Industry Association, 2003. Available from: <http://public.itrs.net>.

[48] C.I. Siettos, A. Armaou, A.G. Makeev, I.G. Kevrekidis, Microscopic/stochastic timesteppers and coarse control: a kinetic Monte Carlo example, AIChE J. 49 (2003) 1922–1926.

[49] C. Theodoropoulos, Y.H. Qian, I.G. Kevrekidis, Course stability and bifurcation analysis using time-steppers: a reaction-diffusion example, Proc. of the National Academy of Sciences 97 (2000) 9840–9843.

[50] B.L. Trout, Car-Parrinello methods in chemical engineering: their scope and potential, Advances in Chemical Engineering 28 (2001) 353–397.

[51] D.G. Vlachos, Multiscale integration hybrid algorithms for homogeneous–heterogeneous reactors, AIChE J. 43 (1997) 3031–3041.

[52] P.R. Westmoreland, P.A. Kollman, A.M. Chaka, P.T. Cummings, K. Morokuma, M. Neurock, E.B. Stechel, P. Vashishta, 2002. Applications of Molecular and Materials Modeling. Technical report, International Technology Research Institute, Baltimore, MD.